Spring Technical Meeting
Eastern States Section of the Combustion Institute
March 6-9, 2024
Athens, Georgia

Ignition characteristics of cellulose hydrochar using in-situ diagnostics

Parvaneh Motiei¹, Matteo Pecchi², James L. Adair², Jillian L. Goldfarb² Jacqueline O'Connor^{1,*}

¹Mechanical Engineering, Pennsylvania State University, University Park, PA USA
² Biological and Environmental Engineering, Cornell University, Ithaca, NY USA
*Corresponding Author Email: jxo22@psu.edu

Abstract: This work investigates the ignition behavior of cellulose hydrochar fuels carbonized at two different temperatures. Particles are burned in a Hencken burner under various O_2/N_2 mixtures where the impacts of ambient temperature and oxygen mole fractions are assessed independently. CH* chemiluminescence imaging and particle image velocimetry are used to characterize the ignition delay time. Results reveal that for both hydrochars ignition delay time is inversely proportional to the surrounding gas temperature. Ignition delay time shows a non-monotonic dependency on O_2 mole fraction. Increasing the O_2 fraction decreases the ignition delay time until O_2 concentration is at a critical value, after which it increases.

Keywords: Hydrochar, Hydrothermal carbonization, Ignition, Biofuel combustion

1 Introduction

World-wide decarbonization pledges are driving a shift towards renewable fuels, including biomass-based fuels [1]. Hydrothermal carbonization (HTC) of biomasses to form hydrochars is a promising method to convert raw biomass into a carbon-intensive solid fuel with lower reactivity and higher enthalpy of combustion than raw biomass [2],[3]. The literature is replete with thermogravimetric analysis studies of hydrochar investigating the impact of HTC temperature and residence time on oxidation and pyrolysis [4]. Despite the growing interest in hydrochar, very little is known about its fundamental combustion properties and limited works have been reported on direct combustion of this solid biofuel [5], [6]. However, a substantial body of literature exists on carbonaceous solid fuel and raw biomass combustion, exploring the effects of particle size, fuel rank, oxidizing atmosphere, diluent agent, and surrounding gas temperature on combustion timescales, ignition temperature, and combustion modes [7]–[11]. In general, combustion experiments show that higher co-flow temperature and O₂ concentration lower the ignition delay time and burnout time The goal of this study is to investigate the ignition delay time of cellulose-derived hydrochars and the impact of O₂ concentrations and co-flow temperature on these delay times.

2 Material and proximate analysis

Two types of cellulose-based hydrochar are synthesized at two different HTC temperatures, 220°C and 250°C. Microcrystalline cellulose (CLS) was sourced from Alfa Aesar and its combustion behavior was characterized in previous work by our groups [12]. Proximate analysis of CLS and both hydrochars, CH250 and CH220, is shown in Figure 1.

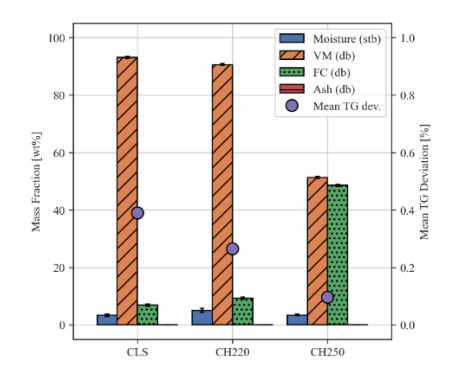


Figure 1. Proximate analysis of cellulose (CLS) and two hydrochars: CH250 and CH220

3 Methods/ Experimental setup

The combustion experiments are performed in a Hencken Burner, (Figure 2(a)), as was done in our previous study [12]. CH* chemiluminescence imaging and particle image velocimetry (PIV) are used to determine the ignition delay time. An overhead schematic of the experiment is shown in Figure 2(b). Images of CH* chemiluminescence emissions of burning particles were captured to identify heat release rate. To quantify the ignition delay time, the particle velocity over the ignition zone was measured by PIV. Details of the diagnostics and data analysis procedures are explained in the previous work [12].

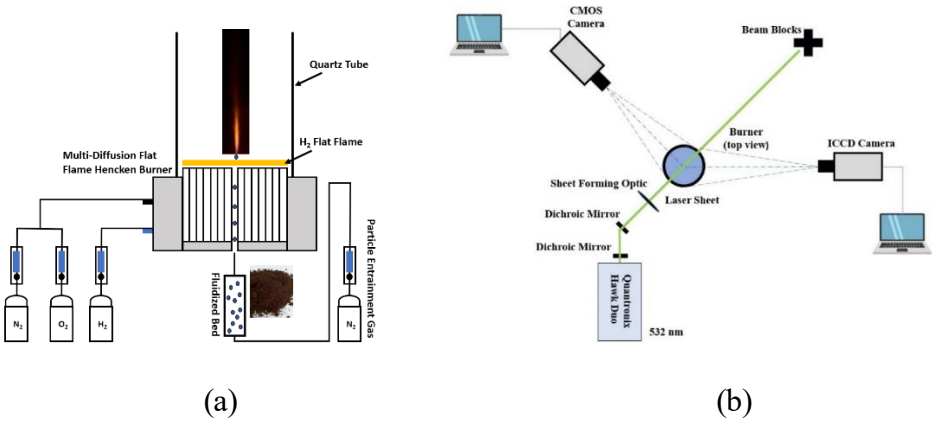


Figure 2. Schematic of (a) experimental rig, (b) simultaneous CH* chemiluminescence and PIV

4 Results and discussion

Combustion behavior of hydrochars is assessed with the test matrix in Table 1. H_2 fuel and O_2/N_2 mixture flow rates are varied in the Hencken burner that different temperature and O_2 mole fractions are achieved while the total mass flow of the co-flow and particles are constant.

Table 1. Test matrix designed for hydrochar

Constant T _{ad} while varying O ₂ concentration in combustion products			Constant O ₂ concentration in combustion products while varying T _{ad}		
φ	$T_{ad}(K)$	O ₂ mole fraction	φ	$T_{ad}(K)$	O ₂ mole fraction
0.7	1645	0.04	0.5	1329	0.06
0.63	1645	0.05	0.52	1430	0.06
0.58	1645	0.06	0.54	1527	0.06

	0.50	1645	0.09	0.56	1618	0.06
	0.42	1645	0.12	0.58	1706	0.06
Ī	0.35	1645	0.17			

Figure 3 shows the centerline intensity profiles along the downstream direction extracted from the time-averaged CH* images for varying temperature with a constant O₂ mole fraction of 0.06. Depending on carbonization level of the hydrochar and surrounding gas temperature, CH* signal profiles exhibit different shapes, which can be attributed to different combustion modes. In all CH250 cases in Figure 3(a), there are two maxima in the CH* signal, suggesting two different combustion modes; previous research suggests that the first peak is the result of gas-phase ignition of volatiles and the second peak is the result heterogeneous combustion of the solid fuel [9]–[11]. However, as the temperature increases, the relative amplitude of the CH* signal during each combustion mode changes. The CH220 CH* profiles, in Figure 3(b), show a change in profile shape and likely combustion mode with temperature. At the lower gas temperatures (1329 K and 1430 K), a single-peak behavior is observed, as was seen with cellulose in our previous study [12]. By raising the surrounding gas temperature above 1430 K, the intensity profiles show a shoulder in the downstream portion of the profile.

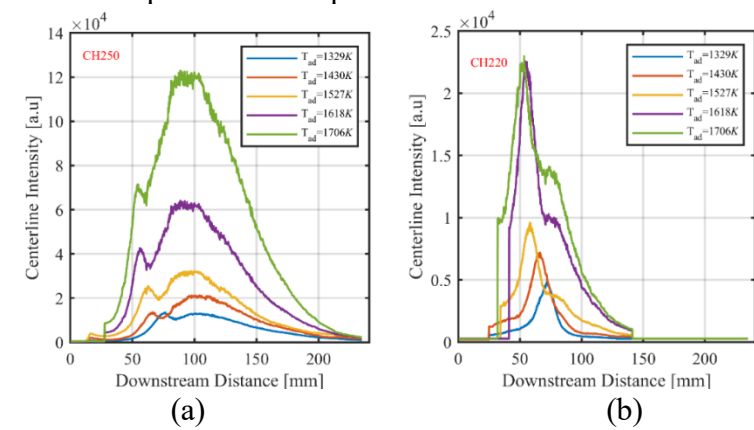


Figure 3. Centerline intensity at different T_{ad} and constant O_2 (a) CH250, (b) CH220

Ignition delay times at different ambient temperatures are shown in Figure 4(a) and (b); the ignition delay is determined from the maximum gradient in the CH* signal.

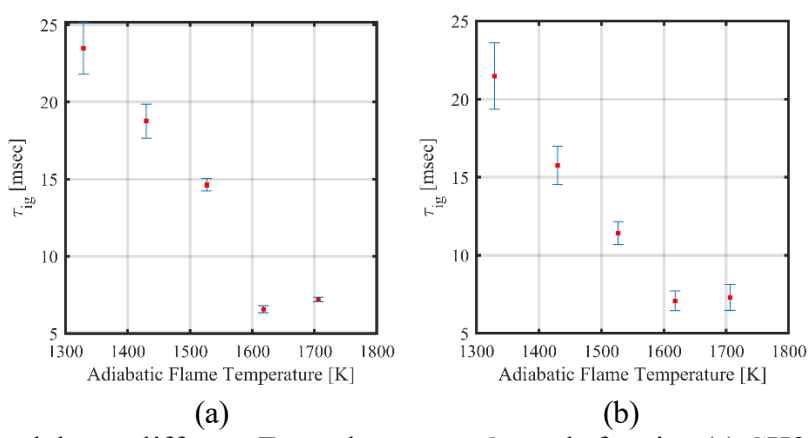


Figure 4. Ignition delay at different T_{ad} and constant O₂ mole fraction (a) CH250, (b) CH220

Both hydrochars show a decreasing trend with increasing gas temperature. Up to 1618 K the ignition delay time for CH250 is higher than CH220, which is consistent with slower oxidation of the more carbonized hydrochar. However, in both hydrochars, the trend at highest temperatures is flattened and the ignition delay times have close magnitudes regardless of carbonization level of hydrochar; similar trends have been seen for other solid fuels [8].

CH* centerline intensity of both hydrochars for constant O₂ mole fraction cases at a constant temperature are shown in Figure 5. Both hydrochars show a change in the shape of the CH* curve with increasing O₂ mole fraction from 0.04-0.17, which implies that combustion mode is oxygen sensitive. The CH* profile of the CH250 at low oxygen levels (0.04-0.06) shows only one peak, whereas a small but repeatable shoulder is present in the higher oxygen levels (0.09-0.17), likely the result of a change in combustion mode.

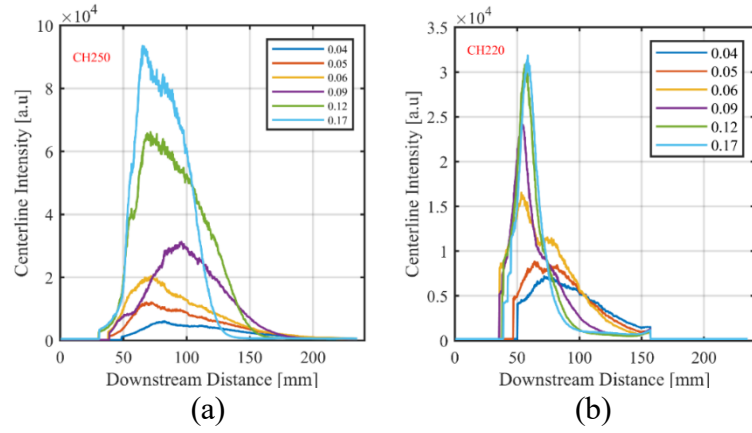


Figure 5. Centerline intensity at different O₂ levels and constant T_{ad} (a) CH250, (b) CH220

Ignition delay times (Figure 6) decrease with increasing the O_2 mole fraction until O_2 reaches a critical value and the combustion mode transition occurs. For O_2 mole fractions above the critical value, the ignition delay time increases with increasing O_2 mole fraction, implying a complex impact of oxygen that needs further investigation. Similar results were observed in previous work [10].

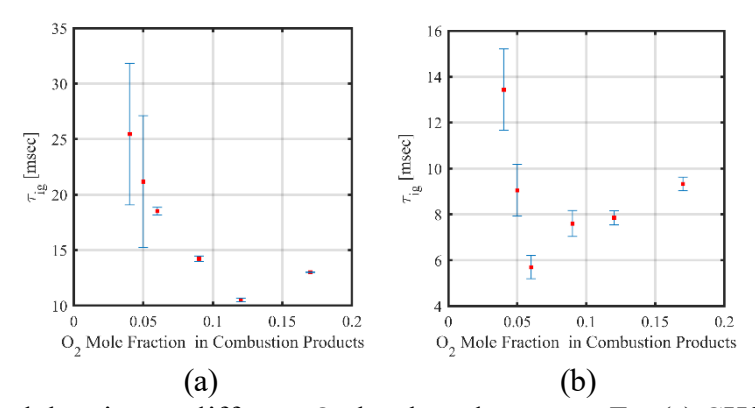


Figure 6. Ignition delay time at different O_2 levels and constant T_{ad} (a) CH250, (b) CH220

5 Conclusions

Cellulose hydrochar particles carbonized at two temperatures were burned in a Hencken burner to characterize the ignition delay time. Results suggest that the ignition mode depends on gas temperature, O₂ mole fraction, and level of carbonization of the fuel. Ignition delay time

decreased with increasing temperature at a constant oxygen level for both levels of char carbonization, but the trends with O₂ mole fraction at a constant temperature is non-monotonic.

6 Acknowledgements

The authors gratefully acknowledge financial support from National Science Foundation (NSF), grant numbers CBET-2031710 and CBET-2031916.

7 References

- [1] R. S. Dhillon and G. von Wuehlisch, "Mitigation of global warming through renewable biomass," *Biomass and bioenergy*, vol. 48, pp. 75–89, 2013.
- [2] X. Dong *et al.*, "Hydrothermal carbonization of millet stalk and dilute-acid-impregnated millet stalk: combustion behaviors of hydrochars by thermogravimetric analysis and a novel mixed-function fitting method," *Fuel*, vol. 273, p. 117734, 2020.
- [3] M. Wilk, M. Śliz, and M. Gajek, "The effects of hydrothermal carbonization operating parameters on high-value hydrochar derived from beet pulp," *Renew. Energy*, vol. 177, pp. 216–228, 2021.
- [4] M. Lucian, M. Volpe, L. Gao, G. Piro, J. L. Goldfarb, and L. Fiori, "Impact of hydrothermal carbonization conditions on the formation of hydrochars and secondary chars from the organic fraction of municipal solid waste," *Fuel*, vol. 233, pp. 257–268, 2018.
- [5] H. Düdder, A. Wütscher, N. Vorobiev, M. Schiemann, V. Scherer, and M. Muhler, "Oxidation characteristics of a cellulose-derived hydrochar in thermogravimetric and laminar flow burner experiments," *Fuel Process. Technol.*, vol. 148, pp. 85–90, 2016.
- [6] Z. Lu, X. Li, J. Jian, and S. Yao, "Flame combustion of single wet-torrefied wood particle: Effects of pretreatment temperature and residence time," *Fuel*, vol. 250, pp. 160–167, 2019.
- [7] R. Khatami and Y. A. Levendis, "On the deduction of single coal particle combustion temperature from three-color optical pyrometry," *Combust. Flame*, vol. 158, no. 9, pp. 1822–1836, 2011.
- [8] G. Simões, D. Magalhães, M. Rabaçal, and M. Costa, "Effect of gas temperature and oxygen concentration on single particle ignition behavior of biomass fuels," *Proc. Combust. Inst.*, vol. 36, no. 2, pp. 2235–2242, 2017, doi: 10.1016/j.proci.2016.06.102.
- [9] A. Adeosun, Z. Xiao, Z. Yang, Q. Yao, and R. L. Axelbaum, "The effects of particle size and reducing-to-oxidizing environment on coal stream ignition," *Combust. Flame*, vol. 195, pp. 282–291, 2018.
- [10] Y. Yuan, S. Li, G. Li, N. Wu, and Q. Yao, "The transition of heterogeneous—homogeneous ignitions of dispersed coal particle streams," *Combust. Flame*, vol. 161, no. 9, pp. 2458–2468, 2014.
- [11] Y. Yuan, S. Li, F. Zhao, Q. Yao, and M. B. Long, "Characterization on heterohomogeneous ignition of pulverized coal particle streams using CH* chemiluminescence and 3 color pyrometry," *Fuel*, vol. 184, pp. 1000–1006, 2016.
- [12] P. Motiei, M. Pecchi, J. L. Adair, J. L. Goldfarb, and J. O'Connor, "Pairing combustion experiments and thermogravimetric analysis to uncover timescales controlling cellulose ignition and burnout in a Hencken burner," *Combust. Flame*, vol. 258, p. 113092, 2023.